

A Novel Leaf Extract of *Sorghum Vulgare* as an Eco-friendly Corrosion Inhibitor for Mild Steel Corrosion in 0.5 M H₂SO₄

**S. Sharma¹, M. Sharma¹, N. Dheer², S. K. Ujjain³,
P. Ahuja³, G. Singh⁴ and R. Kanojia^{*5}**

¹*Department of Chemistry, Faculty of Engineering and Technology, Manav Rachna International Institute of Research and Studies, Haryana, India*

²*Department of Chemistry, Acharya Narendra Dev College, University of Delhi, Delhi, India*

³*Research Initiative for Supra-Materials, Shinshu University, Nagano, Japan*

⁴*Department of Chemistry, University of Delhi, Delhi, India*

⁵*Department of Chemistry, Shivaji College, University of Delhi, Delhi, India*

*Corresponding author. E-mail address: drrajnikanojia@gmail.com

Received 07/11/2021; accepted 25/03/2022

<https://doi.org/10.4152/pea.2023410402>

Abstract

MS effective corrosion inhibition by SVLE has been investigated using electrochemical methods. Tafel polarization measurements suggested that the reaction at the anode occurred with MS dissolution, due to the strong medium aggressiveness, but SVLE addition led to a corrosion IE(%) of 93.6%, at 298 K. SVLE IE(%) still was 86% at an elevated T of 328 K, which was also confirmed by SEM observations that revealed a protective adsorbed film formed by the inhibitor onto the MS surface.

Keywords: SVLE, MS, corrosion, polarization curve and high T IE(%).

Introduction*

Corrosion research has been among most trending study topics in the past few years, due to its diverse usage in constructional and industrial applications [1, 2]. Recently, a study revealed that corrosion causes economic losses of about 2.5 trillion US dollars a year, constituting almost 3.4% of the worldwide GDP [3]. As corrosion is associated with economic and safety issues, it should be highly addressed by the researchers throughout the world.

Metals and alloys are exposed to hostile environments during their industrial usage, including manufacturing, processing and transportation, which accelerate their degradation. In particular, steel and its alloys are the most utilized metals in renowned industries, for different applications, due to their low cost and good mechanical strength, with high thermal and mechanical conductivity [4-6]. However, their practical utility in industries is threatened during cleaning, pickling and oil well oxidization in acidic solutions that corrode them [7, 8]. This natural phenomenon can

* The abbreviations and symbols definitions lists are in pages 283-284.

be minimized to a great extent through the use of corrosion inhibitors. The development of new, in particular, eco-friendly and green corrosion inhibitors is therefore urgently required, for ensuring humankind and environmental safety.

Natural products, such as plant extracts, are highly demanded, due to ecological consciousness and eco-friendly regulations in different fields of science and technology, since they are ecologically acceptable and renewable sources [9-11]. Plant extracts corrosion inhibition activity is correlated to the presence of abundant chemical constituents, such as alkaloids, flavonoids and tannins, which have large potential to prevent corrosion [12, 13]. Alireza et al. have made a comparative study of henna extract and its constituents, namely, gallic and tannic acids, α -D-Glucose and Lawsone, for MS corrosion inhibition in HCl. Henna inhibitor molecules were chemisorbed on the MS surface, but the corrosion inhibition was slightly enhanced by oxygen scavenging [14]. Mohsen et al. have analysed the effect of two oleo-gum resin exudates on MS corrosion inhibition in aggressive media. They acted as mixed-type inhibitors, predominantly controlling corrosion. EIS showed that corrosion was controlled by a charge transfer process [15].

Although many plant extracts have shown potential to mitigate corrosion, no study has yet investigated the effect of harsh conditions, such as high T, on their IE(%).

SVLE, which has been widely used in numerous applications [16], due to its significant nutritional value, lesser water requirements and high adaptability to a broad range of growing conditions, is greatly available. It is expected to show high corrosion IE(%), since it contains phenolic compounds, such as flavonoids [17].

Prompted by SVLE abovementioned properties, the present study aimed to measure the feasibility of using this natural, inexpensive and green corrosion inhibitor. Electrochemical measurement results showed good agreement with the MS surface examination by AFM and SEM. Furthermore, thermodynamic parameters that govern MS corrosion have also been evaluated, and showed SVLE great potential as corrosion inhibitor.

Experimental method

SVLE preparation

50 g of fresh and washed SV leaves were taken and poured into a 100 mL 0.5 M H₂SO₄ solution. This extract was refluxed for 180 min, allowed to cool down at 25 °C, and filtered. Thus, 50% SVLE were obtained. From the proper extract dilution, solutions of 10, 20, 30 and 40% were obtained.

MS specimen preparation

MS specimens (composition: 95.5% Fe, 1.92% C, 0.034% S, 0.165% Si, 0.203% Cu and 0.60% Mn), with 1 x 1 cm² exposed surface area, were encapsulated in an Araldite standard epoxy adhesive, and used as WE for electrochemical measurements, i.e. PDP and EIS measurements. To obtain a MS uniform surface, the exposed surface area was successively abraded with different grades of emery paper (i.e., 220, 400, 800,

1000 and 2000), and degreased with acetone and distilled H₂O, in order to obtain polished coupons for electrochemical experiments.

Electrochemical techniques

SVLE was utilized with four different C: 10, 20, 30 and 40%. A three-electrode assembly cell was used to evaluate T effect on MS corrosion inhibition, at 298, 308, 318 and 328 K. This assembly was then kept in the water bath for 3 h, in order to attain a steady-state and OCP. An electrochemical work station impedance analyzer (CHI 760D) was used for investigations. Tafel plots were performed at a SR of 0.01 mV s⁻¹, in an E range from -0.9 to +0.0 V. Kinetic and activation parameters for adsorption and dissolution processes were then calculated. EIS measurements were performed by using an AC signal, with 5 mV amplitude, at OCP, in the frequency range from 105 to 1 Hz.

Surface characterization

Polished MS coupons were dipped into a 0.5 M H₂SO₄ solution without and with SVLE, in its highest and lowest C of 40 and 10%, for 1 day. MS coupons surface morphology was analyzed using Ziess S-3700 N SEM and Nanosurf Naio AFM, both from Germany.

Results and discussion

PDP study

The MS surface exhibited better corrosion inhibition with SVLE, as demonstrated by electrochemical PDP results from Tafel curves in H₂SO₄ (Fig.1 (a-d)).

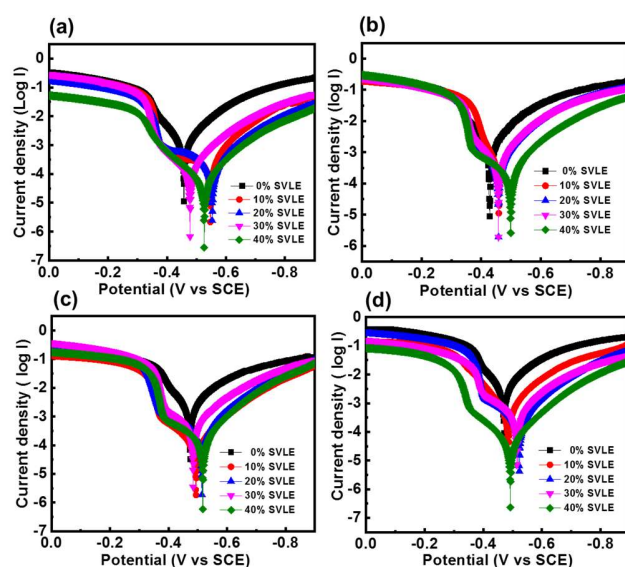


Figure 1. Tafel curves of MS in 0.5 M H₂SO₄ with different SVLE C, at: (a) 298; (b) 308; (c); 318; and (d) 328 K.

Corrosion electrochemical parameters values, such as E_{corr} and I_{corr}, were calculated from Tafel curves (Table 1), following our previous article [18].

Table 1. PDP parameters for MS corrosion in 0.5 M H₂SO₄ with various SVLE C.

T (K)	SVLE C in 0.5 M H ₂ SO ₄ (%)	E _{corr} (mV)	β _c (mV/dec)	β _a (mV/dec)	I _{corr} (mA/cm ²)	IE(%)	θ
298	0	457	114	61	1.017	-	-
	10	547	124	172	0.303	70.14	0.701
	20	553	220	151	0.219	78.46	0.784
	30	478	108	90	0.107	89.40	0.894
	40	526	119	108	0.064	93.65	0.936
308	0	429	116	61	1.267	-	-
	10	458	137	108	0.461	63.58	0.635
	20	459	111	43	0.314	75.21	0.752
	30	458	173	119	0.164	87.04	0.870
	40	502	156	159	0.104	91.74	0.917
318	0	474	144	66	1.984	-	-
	10	489	148	683	0.786	60.36	0.603
	20	514	116	211	0.605	69.46	0.694
	30	484	116	58	0.302	84.74	0.847
	40	517	107	194	0.202	89.80	0.898
328	0	470	133	63	3.009	-	-
	10	487	120	86	1.293	57.02	0.570
	20	523	132	542	1.075	64.27	0.642
	30	514	119	160	0.625	79.21	0.792
	40	504	115	43	0.420	86.02	0.860

IE% values were obtained from PDP, using the following relation [19]:

$$IE(\%) = \frac{I_{\text{corr}} - I_{\text{corr(Inh)}}}{I_{\text{corr}}} \times 100 \quad (1)$$

where I_{corr} and $I_{\text{corr(Inh)}}$ (in uninhibited and inhibited solutions, respectively) were evaluated by the intersection of extrapolated Tafel lines. β_a and β_c varied with the addition of different SVLE C, implying controlled reactions. Additionally, the extract not only hindered cathodic HER, but also retarded MS anodic dissolution. As the extract C increased, inhibition of cathodic and anodic reactions became more visible. Recent studies have shown that, if the inhibited solution E_{corr} values are ± 85 mV with respect to the corrosive medium, the inhibitor is categorized as of the anodic or cathodic types [20-22]. The observed data (Table 1) depict that E_{corr} values varied from 10 to 75 mV, towards less negative values. E_{corr} value did not change significantly by adding SVLE, which indicates that the inhibition behavior was of the mixed type, but with a slight predominance towards the cathodic direction, at lower C. A prominent decreasing trend in I_{corr} values was observed with SVLE in H₂SO₄. I_{corr} values decreased with higher SVLE C, and increased with a rise in T, which indicates that the extract is an effective inhibitor in higher C for MS corrosion in H₂SO₄, at lower T. It is noticeable that, at SVLE lowest and highest C (10 and 40%), IE(%) was 70.1 and 93.6%, respectively. This could be due to the better θ accomplished by SVLE molecules onto the MS surface [23]. Further, SVLE IE(%) showed a decreasing trend with an increase in T, but it still was 86%, at 328 K (Fig. 1). A similar decreasing trend in IE(%) was seen for the other three C.

According to Le-Chatelier’s principle, the adsorption exothermic reaction started to move in the opposite direction, leading to the extract molecules desorption from the MS surface, as the system T increased [24]. Therefore, θ by the extract molecules decreased with increasing T, thereby diminishing IE(%). These results suggested that SVLE adhered onto the MS surface, which hindered anodic reaction kinetics and retarded MS dissolution, even under high T conditions.

Adsorption isotherm

θ is an important parameter for studying the adsorption process involved during corrosion inhibition. θ values for various SVLE C in 0.5 M H₂SO₄ were evaluated from PDP studies, in the T range from 298 to 328 K (Table 1). The best correlation between the electrochemical investigational outcomes and adsorption functions was evaluated by the Langmuir’s adsorption isotherm, according to the relation [25]:

$$\frac{C}{\theta} = \frac{1}{K_{ads}} + C \quad (2)$$

The plot of C/ θ , as a function of SVLE C in H₂SO₄, with a raise in T from 298 to 328 K, exhibits a straight line (Fig. 2).

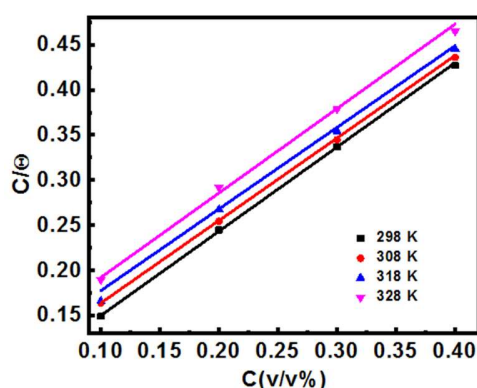


Figure 2. Langmuir’s adsorption isotherm for SVLE molecules adsorbed onto the MS surface in 0.5 M H₂SO₄, at various T.

The linear regression parameters obtained at different T are given in Table 2.

Table 2. Linear regression parameters for SVLE.

T	Intercept	Slope	R ²
298 K	0.056	0.934	0.993
308 K	0.072	0.914	0.994
318 K	0.086	0.905	0.979
328 K	0.098	0.936	0.976

It is apparent, from the results, that all R² values were approximately equal to 1, which signifies that SVLE molecules that were adsorbed onto the MS surface followed the

Langmuir's adsorption isotherm. Calculations for the adsorption process from the straight line obtained by plotting C/θ versus C (Fig. 2) show the correlation between K_{ads} and $\Delta G_{\text{ads}}^{\circ}$ [26].

$$\Delta G_{\text{ads}}^{\circ} = -2.303 RT \log(55.5 K_{\text{ads}}) \quad (3)$$

The determined thermodynamic parameters are shown in Table 3.

Table 3. Thermodynamic parameters obtained for SVLE molecules adsorbed onto the MS surface, at various T.

T (K)	K_{ads} (L/mol)	$\Delta G_{\text{ads}}^{\circ}$ (kJ/mol)	$\Delta H_{\text{ads}}^{\circ}$ (kJ/mol)	$\Delta S_{\text{ads}}^{\circ}$ (kJ/mol)
298	17.71	-17.07		23.69
308	13.84	-17.01	-10.01	22.72
318	11.50	-17.07		22.20
328	10.15	-17.27		22.13

It is clearly indicated that K_{ads} decreased slightly as T increased, which confirms that SVLE molecules were strongly adsorbed onto the MS surface. Adsorbed SVLE molecules tended to desorb from the MS surface with elevated T, and IE(%) also decreased [27, 28].

Further, $\Delta H_{\text{ads}}^{\circ}$ was evaluated from the plot of K_{ads} log variation against $1/T$ (Fig. 3).

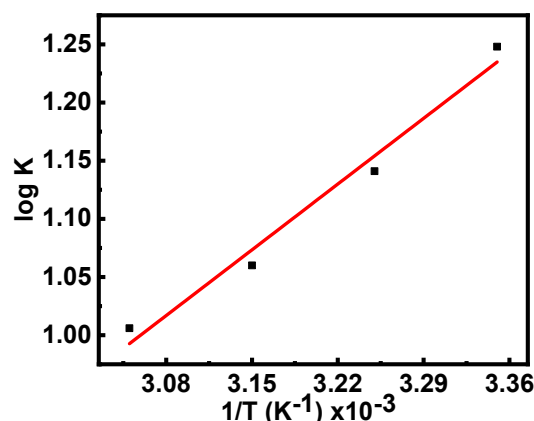


Figure 3. Plot of K_{ads} log variation vs. $1/T$ for SVLE.

$\Delta H_{\text{ads}}^{\circ}$ negative value (-10.01 kJ/mol) indicates that SVLE molecules adsorption onto the MS surface was a spontaneous and exothermic process [29, 30], which concurs with the decrease in IE(%) at elevated T. Usually, $\Delta G_{\text{ads}}^{\circ}$ values up to -20 kJ/mol signify that the interaction between the inhibitor and the charged metal was electrostatic [31, 32]. Calculated $\Delta G_{\text{ads}}^{\circ}$ values ranged from -17.01 to -17.27 kJ/mol, which means that SVLE physisorption occurred onto the MS surface immersed in H_2SO_4 [33, 34].

Additionally, $\Delta S_{\text{ads}}^{\circ}$ positive values indicate an increase in the adsorption process entropy, which can be explained by considering a substitution mechanism. When

SVLE molecules in the aqueous phase are getting adsorbed onto the MS surface, they and H₂O molecules at the electrode surface swap sites with each other. This way, the inhibitor molecules adsorption takes place when H₂O molecules simultaneously leave their position and enter in to the solution. $\Delta S^{\circ}_{\text{ads}}$ and desorption process algebraic sum create a net positive ΔS change. ΔS value reveals that SVLE molecules adsorption was not reversible, which substantiates the inhibitor good thermal stability [35].

Arrhenius equation was used to calculate MS E_a in H₂SO₄, which was given by equation [36]:

$$\ln I_{\text{corr}} = \frac{-E_a}{RT} + \ln A \quad (4)$$

where A is the Arrhenius factor and R is the universal gas constant. Fig. 4 presents the Arrhenius plots of I_{corr} natural logarithm versus T reciprocal.

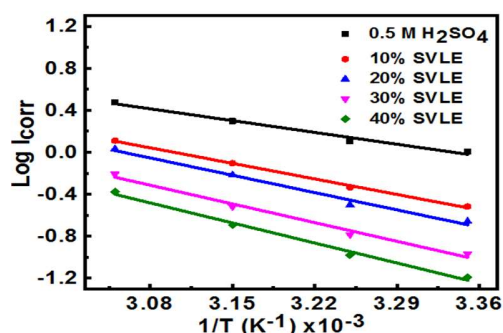


Figure 4. $\ln I_{\text{corr}}$ versus $1/T$ for MS dissolution in 0.5 M H₂SO₄.

CR decreased in SVLE presence, with a marked increase in E_a values (Table 4).

Table 4. E_a values for MS corrosion in solutions without and with SVLE.

SVLE C in 0.5 M H ₂ SO ₄ (%)	E_a (kJ/mol)
0	13.37
10	17.61
20	19.60
30	21.16
40	22.68

E_a was found to be 22.68 and 17.61 kJ/mol, at 40 and 10% SVLE, respectively. As already reported, based on E_a value, the adsorption phenomena can be classified into physisorption ($E_a < 40$ kJ/mol) and chemisorption ($E_a > 80$ kJ/mol) [37]. This confirms that SVLE was physically adsorbed onto the MS surface, acting as a protective coverage against H₂SO₄.

EIS

EIS measurements were conducted for examining the corrosion process quantitative kinetics. The impedance measurements were carried out in a 0.5 M H₂SO₄ solution

without and with SVLE, at 40, 30, 20 and 10%, in a three electrode cell assembly, as shown in Fig. 5(a).

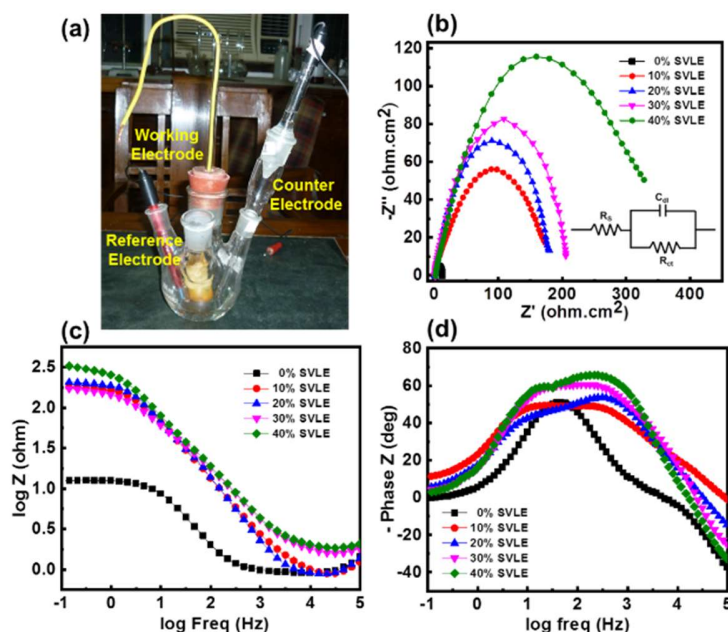


Figure 5. (a) Three electrode cell assembly showing MS WE, calomel RE and Pt CE in 0.5 M H₂SO₄ that acted as electrolyte or corrosive medium. EIS parameters: (b) Nyquist (inset shows an equivalent circuit model); (c) Bode; and (d) phase angle-frequency plots in a 0.5 M H₂SO₄ solution without and with various SVLE C, at 298 K.

EIS results are presented in the form of Nyquist and Bode plots (Fig. 5(b) and (c)). Nyquist plot possesses a depressed capacitive loop, which is attributed to a single time constant for H₂SO₄ and SVLE solutions, at 298 K. The diameter of these semicircle increased with higher SVLE C, indicating the effective extract inhibition of MS surface corrosion. This single capacitive loop suggests that MS corrosion was primarily controlled by a charge transfer process. However, the deviation from a perfect semicircle is attributed to porosity in mass transport effects, and frequency dispersion and relaxation [38].

The Bode plot represents an increase in the absolute impedance value $|Z|$, at low frequencies, after MS preliminary treatment with SVLE. An increase in the extract C, from 10 to 40%, led to its effective adsorption onto the MS surface, which protected it more effectively from corrosion. Fig. 5(d) is in agreement with Bode plot, showing a continuous well-pronounced phase angle shift at higher frequencies, which indicates that the protection barrier was less stable. It also suggests that the pseudo-capacitive film has been formed onto the MS surface, inhibiting its corrosion in H₂SO₄ [39].

Impedance parameters, such as C_{dl} , R_{ct} , frequency at maximum Z''_{max} (f_{max}) and IE(%), are listed in Table 5. Further, IE(%) was calculated by using the following formula [40]:

$$IE(\%) = \frac{R_{ct}(\text{Extract}) - R_{ct}(\text{Acid})}{R_{ct}(\text{Extract})} \times 100 \quad (5)$$

where $R_{ct}(\text{Extract})$ and $R_{ct}(\text{Acid})$ are charge transfer resistances with and without SVLE, respectively.

From Table 5, it was noted that, with higher SVLE C, R_{ct} increased, and its highest value, obtained with 40% SVLE, was $396.65 \Omega/\text{cm}^2$, and IE(%) was 93.4%. 30% SVLE gave a R_{ct} value of $191.79 \Omega/\text{cm}^2$, with an IE(%) of 86.4%. A lower SVLE C produced decreased R_{ct} values of 127.74 and $88.83 \Omega/\text{cm}^2$, with an IE(%) of 79.5 and 70.6%, respectively.

Table 5. Electrochemical impedance parameters in 0.5 M H_2SO_4 without and with different SVLE C, at 298 K.

Extract	C (%)	R_{ct} (Ω/cm^2)	C_{dl} ($\mu\text{F}/\text{cm}^2$)	F_{max}	IE%	θ	Phase angle α°
H_2SO_4	0.5	26.06	369.67	9.03	-	-	-
SVLE	40	396.65	4.50	89.16	93.42	0.934	63
	30	191.79	11.70	70.93	86.41	0.864	57
	20	127.74	31.23	39.90	79.59	0.795	46
	10	88.83	77.42	23.15	70.66	0.706	43

On the contrary, SVLE absence gave a very lower R_{ct} value of $26.06 \Omega/\text{cm}^2$. It is noticeable from the results that C_{dl} decreased with an increase in R_{ct} . Due to C_{dl} reduction, it can be ascertained that SVLE molecules were adsorbed onto the MS surface, forming a protective layer on the metal-electrolyte surface [41, 42].

Morphological characterization

Complimentarily, AFM micrographs investigated MS topography and surface properties. In the present study, MSR was quantitatively evaluated (Table 6), in order to predict its morphological changes after SVLE addition.

Table 6. AFM roughness data for the MS surface in 0.5 M H_2SO_4 without and with SVLE.

Extract	C (%)	SR average area (nm)
Polished MS	-	125.54
H_2SO_4	0.5	964.47
SVLE	10	328.97
SVLE	40	204.00

The plain MS surface morphology shown in Fig. 6(a) clearly displays almost no roughness. The micrographs further revealed that the MS surface immersed in H_2SO_4 with 10 and 40% SVLE was smoother and less damaged than the one dipped into the blank aggressive medium (Fig. 6(b-d)). Fig. 6(b) and Table 6 show the corroded MS bumpy structure, with an average roughness of 964.47 nm, without SVLE. However, a smoother MS surface morphology was obtained with higher (40%) than with lower (10%) SVLE C, as can be noticed by their MSR values of 204.0 and 328.97 nm, respectively.

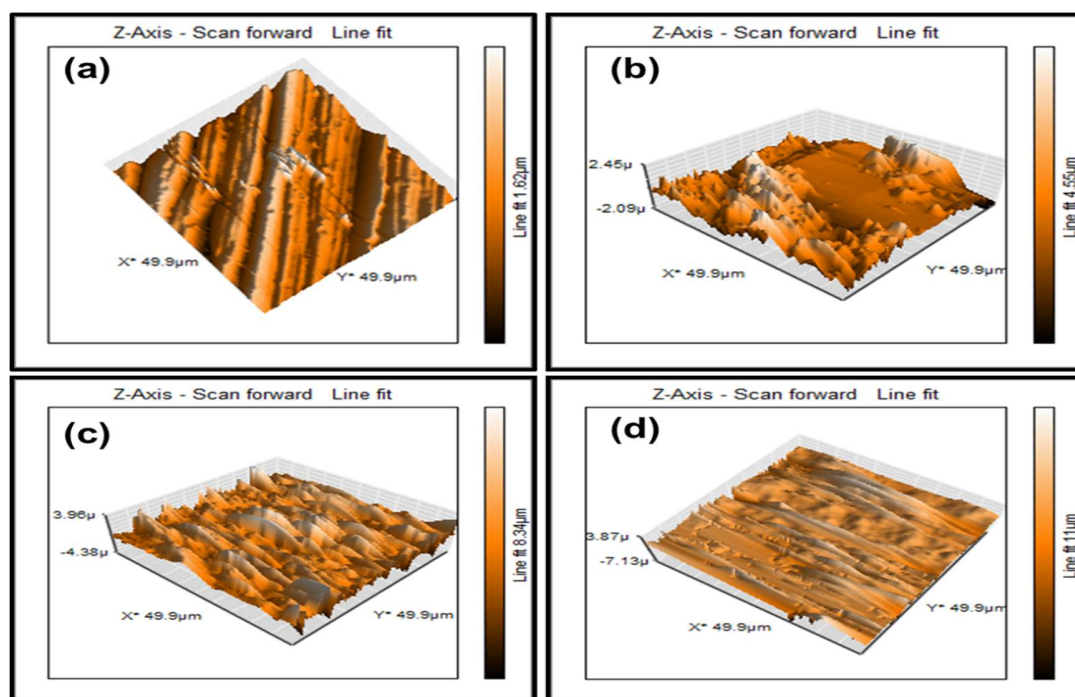


Figure 6. AFM images with surface height for MS: (a) polished surface; (b) in 0.5 M H_2SO_4 ; (c) in 10% SVLE; and (d) in 40% SVLE.

In addition to this, SEM micrographs (Fig. 7) investigated 10 and 40% SVLE molecules interaction with the MS surface in H_2SO_4 (Fig. 7(c-d)).

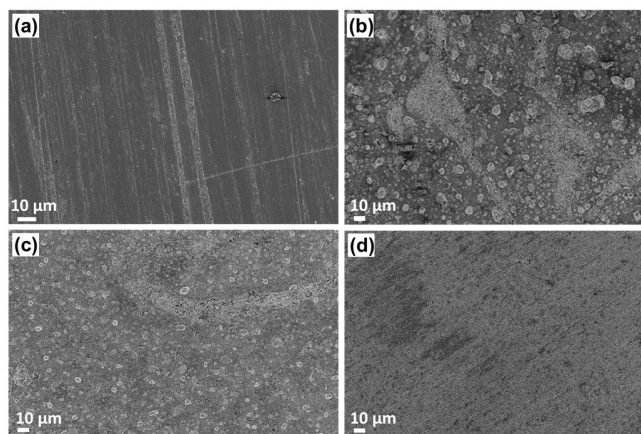


Figure 7. SEM micrographs for MS surface: (a) polished; (b) in 0.5 M H_2SO_4 ; (c) with 10% SVLE; and (d) with 40% SVLE.

As shown in the micrographs, SVLE mitigated MS corrosion process in H_2SO_4 . The SEM image of the extract lower C (10% (Fig. 7(c)) displayed MS surface slight roughness, with some cracks and pits, while, at a higher C (40 % (Fig. 7 (d))), it is as smooth as the polished one shown in Fig. 7(a).

Conclusions

SVLE is the most abundant, economical, easy processable, effective and efficient eco-friendly inhibitor for MS corrosion in aggressive media. Electrochemical measurements have showed that SVLE retarded MS corrosion in 0.5 M H₂SO₄, with high IE(%) of 93.6%, which was 86%, even at elevated T. SVLE is a mixed type inhibitor, with a slight predominance towards the cathodic direction, at lower C. SVLE molecules absorbed onto the MS surface followed Langmuir's isotherm. ΔG°_{ads} values signify that SVLE mechanism of adsorption onto the MS surface in a H₂SO₄ solution involved physisorption. IE(%) data obtained from EIS and PDP measurements showed analogous results, in agreement with the diminished MSR shown by AFM and SEM micrographs.

Acknowledgements

Authors thank USIC, DU for characterization facility.

Competing financial interests

The authors declare no competing financial interests.

Authors' contributions

S. Sharma: was in the main charge of this research; conceived the idea and supervised the whole project; performed the experiments; analyzed the experimental data; prepared the paper. **M. Sharma:** prepared the paper. **N. Dheer:** discussed the results; helped in the analysis; edited the paper. **S. K. Ujjain:** discussed the results; helped in the analysis; edited the paper. **P. Ahuja:** discussed the results; helped in the analysis; edited the paper. **G. Singh:** edited the paper. **R. Kanojia:** conceived the idea; supervised the whole project; prepared and edited the paper.

Abbreviations

AC: alternating current

AFM: atomic force microscope

C: concentration

C_{dl}: double layer capacitance

CE: counter electrode

CR: corrosion rate

E: electric potential

E_a: activation energy

E_{corr}: corrosion potential

EIS: electrochemical impedance spectroscopy

HCl: hydrochloric acid

HER: hydrogen evolution reaction

I_{corr}: corrosion current density

IE(%): inhibition efficiency

K_{ads}: adsorption equilibrium constant
MS: mild steel
MSR: metal surface roughness
OCP: open circuit potential
PDP: potentiodynamic polarization
R²: regression coefficient
R_{ct}: charge transfer resistance
RE: reference electrode
SEM: scanning electron microscope
SR: scan rate
SVLE: *Sorghum vulgare* leaf extract
T: temperature
WE: working electrode

Symbols definitions

β_a: anodic Tafel line
β_c: cathodic Tafel line
ΔG^o_{ads}: free energy of adsorption
ΔH^o_{ads}: enthalpy of adsorption
ΔS: entropy of activation
ΔS^o_{ads}: entropy of adsorption
θ: surface coverage

References

1. Elaheh K, Seyed YA, Mehrad M et al. In situ synthesis, electrochemical and quantum chemical analysis of an amino acid-derived ionic liquid inhibitor for corrosion protection of mild steel in 1 M HCl solution. *Corros. Sci.* 2016;112:73-85. <https://doi.org/10.1016/j.corsci.2016.07.015>
2. Eiman A, Mohammad RK, Ghasem B et al. *Glycyrrhiza glabra* leaves extract as a green corrosion inhibitor for mild steel in 1 M hydrochloric acid solution: Experimental, molecular dynamics, Monte Carlo and quantum mechanics study. *J. Mol. Liq.* 2018;255:185-198. <https://doi.org/10.1016/j.molliq.2018.01.144>
3. Chandrabhan V, Eno EE, Indra B et al. An overview on plant extracts as environmental sustainable and green corrosion inhibitors for metals and alloys in aggressive corrosive media. *J. Mol. Liq.* 2018;266:577-590. <https://doi.org/10.1016/j.molliq.2018.06.110>
4. Markus VLDS, Everton DBP, Almir S. *Syzygium cumini* leaf extract as an eco-friendly corrosion inhibitor for carbon steel in acidic medium. *J Taiwan Inst Chem Eng.* 2021;129:342-349. <https://doi.org/10.1016/j.jtice.2021.09.026>
5. Shangwei L, Xin T, Wenjia C et al. How the transitions in iron and steel and construction material industries impact China's CO₂ emissions: Comprehensive analysis from an inter-sector linked perspective. *Appl Energy.* 2018;211:64-75. <https://doi.org/10.1016/j.apenergy.2017.11.040>

6. Jose MCA, Andre CS, Julian MA. Energy and material efficiency of steel powder metallurgy. Powder Technol. 2018;328(39):329-336. <https://doi.org/10.1016/j.powtec.2018.01.009>
7. Mayakrishnan P, Seung-Hyun K, Venkatesen H et al. *Rhus verniciflua* as a green corrosion inhibitor for mild steel in 1 M H₂SO₄. RSC Adv. 2016;6:57144-57153. <https://doi.org/10.1039/C6RA09637A>
8. Mohamed MB, Samia C, Chouchane T et al. Inhibition Efficiency of Cinnamon Oil as a Green Corrosion Inhibitor. J Bio Tribo Corros. 2019;5:28. <https://doi.org/10.1007/s40735-019-0221-0>
9. Anees AK, Mustafa MK, Rana AA et al. Theoretical evaluation of *Citrus aurantium* leaf extract as green inhibitor for chemical and biological corrosion of mild steel in acidic solution: Statistical, molecular dynamics, docking and quantum mechanics study. J Mol Liq. 2021;343:116978. <https://doi.org/10.1016/j.molliq.2021.116978>
10. Bhawsar J, Jain PK, Jain P. Experimental and computational studies of *Nicotiana tabacum* leaves extract as green corrosion inhibitor for mild steel in acidic medium. Alexandria Eng J. 2015;54(3):769-775. <https://doi.org/10.1016/j.aej.2015.03.022>
11. Patricia EA, Adriana N, Claudio AG et al. *Rollinia occidentalis* extract as green corrosion inhibitor for carbon steel in HCl solution. J Ind Eng Chem. 2018;58:92-99. <https://doi.org/10.1016/j.jiec.2017.09.012>
12. Akhil S, Dwarika P, Rajesh H et al. Use of *Sida cordifolia* extract as green corrosion inhibitor for mild steel in 0.5 M H₂SO₄. J Environ Chem Eng. 2018;6(1):694-700. <https://doi.org/10.1016/j.jece.2017.12.064>
13. Marwa BH, Samar A, Naceur E et al. Olive leaf extract as a green corrosion inhibitor of reinforced concrete contaminated with seawater. Arabian J Chem. 2020;13(3):4846-4856. <https://doi.org/10.1016/j.arabjc.2020.01.016>
14. Alireza O, Seyyed MH, Mahmoud P et al. Corrosion Inhibition of mild steel in 1 M HCl solution by henna extract: A comparative study of the inhibition by henna and its constituents (Lawson, Gallic acid, α -D-Glucose and Tannic acid). Corros Sci. 2009;51:1935-1949. <https://doi.org/10.1016/j.corsci.2009.05.024>
15. Mohsen B, Sayed MG, Maryam K et al. The effect of two oleo-gum resin exudate from *Ferula assa-foetida* and *Dorema ammoniacum* on mild steel corrosion in acidic media. Corros Sci. 2011;53:2489-2501. <https://doi.org/10.1016/j.corsci.2011.04.005>
16. Grace B, Kenneth EK, Paul AS et al. Sensory characteristics of grain sorghum hybrids with potential for use in human food. Cereal Chem. 2001;78(6):693-700. <https://doi.org/10.1094/CCHEM.2001.78.6.693>
17. Arun GK, Venkatesh RS, Vijaya R. Nutritional and rheological properties of sorghum. Int J Food Prop. 2009;12(1):55-69. <https://doi.org/10.1080/10942910802252148>
18. Rajni K, Gurmeet S. An interesting and efficient organic corrosion inhibitor for mild steel in acidic medium. Surf Eng. 2005;21:180-186. <https://doi.org/10.1179/174329405X49985>
19. Harish K, Vikas Y, Anu K. Adsorption, corrosion inhibition mechanism, and computational studies of *Azadirachta indica* extract for protecting mild steel: Sustainable and green approach. J Phys Chem Solids. 2022;165:110690. <https://doi.org/10.1016/j.jpcs.2022.110690>

20. Le TT, Nguyen SH, Phan MQB et al. Combined experimental and computational studies on corrosion inhibition of *Houttuynia cordata* leaf extract for steel in HCl medium. J Mol Liq. 2020;315:113787. <https://doi.org/10.1016/j.molliq.2020.113787>
21. Xiang G, Caicai Z, Haifeng L et al. Influence of phytic acid on the corrosion behavior of iron under acidic and neutral conditions. Electrochim Acta. 2014;150(20):188-196. <https://doi.org/10.1016/j.electacta.2014.09.160>
22. Chaitra TK, Kikkeri NM, Harmesh CT. Thermodynamic, electrochemical and quantum chemical evaluation of some triazole Schiff bases as mild steel corrosion inhibitors in acid media. J Mol Liq. 2015;211:1026-1038. <https://doi.org/10.1016/j.molliq.2015.08.031>
23. Ashassi-Sorkhabi H, Shabani B, Aligholipour B et al. The effect of some Schiff bases on the corrosion of aluminium in hydrochloric acid solution. Appl Surf Sci. 2006;252(12):4039-4047. <https://doi.org/10.1016/j.apsusc.2005.02.148>
24. Michae LN, William CH, Boris LTL. Is the adsorption of soil organic matter to haematite (α -Fe₂O₃) temperature dependent? Eur J Soil Sci. 2018;69 (5):892-901. <https://doi.org/10.1111/ejss.12694>
25. Gülsen A. Inhibitor effect of N,N -methylenediacylamide on corrosion behavior of mild steel in 0.5 M HCl. Mater Chem Phys.2008;112(1):234-238. <https://doi.org/10.1016/j.matchemphys.2008.05.036>
26. Mohammad M, Megha B, Yasmina EA. Corrosion mitigation of mild steel in acidic medium using *Lagerstroemia speciosa* leaf extract: A combined experimental and theoretical approach. J Mol Liq. 2019;286(20):110890. <https://doi.org/10.1016/j.molliq.2019.110890>
27. Xianghong L, Shuduan D, Hui F et al. Adsorption and inhibition effect of 6-benzylaminopurine on cold rolled steel in 1.0 M HCl. Electrochim Acta. 2009;54(16):4089-4098. <https://doi.org/10.1016/j.electacta.2009.02.084>
28. Xianghong L, Guannan M. Tween-40 as corrosion inhibitor for cold rolled steel in sulphuric acid: weight loss study, electrochemical characterization and AFM. Appl Surf Sci. 2005;252(5):1254-1265. <https://doi.org/10.1016/j.apsusc.2005.02.118>
29. Ramananda SM, Vivek S, Gurmeet S. *Musa Paradisiaca* Extract as a Green Inhibitor for Corrosion of Mild Steel in 0.5 M Sulphuric Acid Solution. Port Electrochim Acta 2011;29(6):405-417. <https://doi.org/10.4152/pea.201106405>
30. Mohamed EF, Hafida A, Avni B et al. Insight into the corrosion inhibition of new bisquinolin-8-ols derivatives as highly efficient inhibitors for C35E steel in 0.5 M H₂SO₄. J Mol Liq. 2021;342:117333. <https://doi.org/10.1016/j.molliq.2021.117333>
31. Fouad B, Mounim L et al. Thermodynamic characterization of metal dissolution and inhibitor absorption processes in mild steel/ 2,5 bis (n- thienyl)- 1,3,4- thiadiazoles/hydrochloric acid system. Corros Sci. 2005;47(12):2915-2931. <https://doi.org/10.1016/j.corsci.2005.05.034>
32. Saliyan VR, Airody VA. N-[4-(diethylamino)benzylidene]-3- {[8-(trifluoromethyl) quinolin-4-yl]thio}propano hydrazide) as an effective inhibitor of mild steel corrosion in acid media. Mater Chem Phys. 2009;115: 618-627. <https://doi.org/10.1016/j.matchemphys.2009.01.024>
33. Helen LYS, Afidah AR, Chee YG et al. *Aquilaria subintergra* leaves extracts as sustainable mild steel corrosion inhibitors in HCl. Measurement. 2017;109:334-345. <https://doi.org/10.1016/j.measurement.2017.05.045>

34. Neelu D, Rajni K, Gurmeet S. et al. 4(2-Pyridylazo) Resorcinol as Effective Corrosion Inhibitor for Mild Steel in 0.5M H₂SO₄. Surf Eng. 2007;23(3):187-193. <https://doi.org/10.1179/174329407X174470>
35. Xianghong L, Shuduan D, Hui F et al. Inhibition effect of 6-benzylaminopurine on the corrosion of cold rolled steel in H₂SO₄ solution. Corros Sci.2009;51:620-634. <https://doi.org/10.1016/j.corsci.2008.12.021>
36. Roland TL, Olukeye T. Corrosion inhibition properties of the synergistic effect of 4-hydroxy-3-methoxybenzaldehyde and hexadecyltrimethylammoniumbromide on mild steel in dilute acid solutions. J King Saud Univ Eng Sci. 2018;30(4):384-390. <https://doi.org/10.1016/j.jksues.2016.10.001>
37. Orubite KO, Oforka NC. Inhibition of the corrosion of mild steel in HCl solutions by the extracts of leaves of *Nypa fruticans* Wurmb. Mater Lett. 2004;58(11):1768-1772. <https://doi.org/10.1016/j.matlet.2003.11.030>
38. Chandrabhan V, Eno EE, Indra B et al. 5- (Phenylthio)-3H-pyrrole-4-carbonitriles as effective corrosion inhibitors for mild steel in 1 M HCl: Experimental and theoretical investigation. J Mol Liq. 2015;212:209-218. <https://doi.org/10.1016/j.molliq.2015.09.009>
39. Yujie Q, Shengtao Z, Bochuan T et al. Evaluation of Ginkgo leaf extract as an ecofriendly corrosion inhibitor of X70 steel in HCl solution. Corros Sci. 2018;133(1):6-16. <https://doi.org/10.1016/j.corsci.2018.01.008>
40. Mahendra Y, Tarun KS, Taniya P. Amino acid compounds as eco- friendly corrosion inhibitor for N80 steel in HCl solution: Electrochemical and theoretical approaches. J Mol Liq. 2015;212:731-738. <https://doi.org/10.1016/j.molliq.2015.10.021>
41. Ambrish S, Yuanhua L, Songsong C et al. Electrochemical and surface studies of some porphines as corrosion inhibitor for J55 steel in sweet corrosion environment. Appl Surf Sci. 2015;359: 331-339.
42. Mukta S, Gurmeet S. Effect of Brij 35 on mild steel corrosion in acidic medium. Indian J Chem Technol. 2011;18:351-356. <https://doi.org/10.1016/j.apsusc.2015.10.129>